Rev. Int. Contam. Ambie. 30 (3) 317-329, 2014

ELECTROMAGNETIC METHODS APPLICATION FOR CHARACTERIZING A SITE CONTAMINATED BY LEACHATES

Salvador Isidro BELMONTE-JIMÉNEZ[1]*, Alberto BORTOLOTTI-VILLALOBOS[1], José Óscar CAMPOS-ENRÍQUEZ[2], Marco Antonio PÉREZ-FLORES[3], Omar DELGADO-RODRÍGUEZ[4] and María de los Ángeles LADRÓN DE GUEVARA-TORRES[1]

[1] Centro Interdisciplinario de Investigación para el Desarollo Integral Regional-Oaxaca, Instituto Politécnico Nacional, Hornos 1003, Col. Noche Buena, Santa Cruz Xoxocotlán, Oaxaca, México. C.P. 71230
[2] Instituto de Geofisica, Universidad Nacional Autónoma de México, Coyoacán, 04510, México D.F., México
[3] Departamento de Geofísica de Exploración, Centro de Investigación Científica y Educación Superior de Ensenada, Carr. Ensenada-Tijuana, 3918, Zona Playitas, Ensenada, Baja California, México. C.P. 22860
[4] Instituto Mexicano del Petroleo, Eje Central Lázaro Cárdenas Norte 152, San Bartolo Atepehuacan, 07730, México DF., México
*Autor de correspondencia; salvador.belmonte.j@gmail.com

(Recibido diciembre 2013; aceptado junio 2014)

Key words: contamination, geophysical methods VLF and LIN, electric conductivity, landfill

ABSTRACT

Two electromagnetic geophysical methods, very low frequency (VLF) and low induction number coils (EM-LIN) were used to obtain the response to the presence of leachates from a waste disposal site used for more than 24 years, covering an area of 0.16 km^2. This landfill is located in fractured shale and sandstone associated with the Oaxaca Fault. The study was performed on six profiles, four of which were common to both methods, with lengths of 325, 320, 300 and 645 m, in two others only the VLF method was used. The interpretation of VLF data using the Hjelt and Karous filter resulted in current density sections. The current density variation was assumed to indicate the presence of fractures, along which the infiltration of leachate takes place. The interpretation of EM-LIN data provided two-dimensional models showing the distribution of the conductivity of the subsoil. The integration of these results shows a main conductive anomalous zone in the southeastern part of the landfill that increases in thickness towards the middle and with a depth up to 30-40 m. Correlation with natural surface runoff enables to infer that the conductive anomalous body indicates the presence of leachates. Both electromagnetic methods provided a good response in fractured zones.

Palabras clave: contaminación, métodos geofísicos VLF y LIN, conductividad eléctrica, tiradero de basura

RESUMEN

Se utilizaron dos métodos geofísicos electromagnéticos, frecuencia muy baja (VLF, por sus siglas en inglés) y bobinas a bajo número de inducción (EM-LIN, por sus siglas en inglés), para estudiar la presencia de lixiviados de un sitio de disposición de residuos sólidos municipales, el cual opera desde hace más de 24 años y cuya superficie es de 0.16 km^2. El tiradero se encuentra en un medio cuyo fracturamiento está asociado con la Falla Oaxaca. El basamento del tiradero está constituido por lutita y arenisca. El estudio

se realizó en seis perfiles de los cuales cuatro fueron comunes para ambos métodos, con longitudes de 325, 320, 300 y 645 m, y dos más, únicamente usando el método VLF. La interpretación de los datos VLF utilizando el filtro de Karous y Hjelt dio como resultado secciones que indican alta densidad de corriente interpretadas como asociadas a fracturas que favorecen la infiltración de los lixiviados. La interpretación de los datos de EM-LIN brinda modelos bidimensionales que muestran la distribución de la conductividad del subsuelo. La integración de estos resultados indica una zona anómala conductora principal en la parte sureste del tiradero que, de acuerdo a su forma geométrica, se incrementa hacia la parte central del mismo y se observa hasta una profundidad de entre 30 y 40 m, coincidiendo con la zona por donde ocurre el escurrimiento superficial natural a lo largo del cual fluyen los lixiviados, y que han aprovechado algunas fracturas para infiltrase, infiriéndose que las zonas anómalas detectadas son debidas a la presencia de estos contaminantes. Ambos métodos electromagnéticos han proporcionado buena respuesta en un medio fracturado.

INTRODUCTION

A study was conducted in a landfill, located about 15 km to the south of Oaxaca city, along the road from Oaxaca City to Puerto Angel, in the District of Zaachila (**Fig. 1**), where more than 500 tons of wastes per day are deposited. This site represents an important environmental problem because of the presence of leachates that seep into the ground, contaminating the surface water and the local aquifer. Due to the need for fresh water, people dig shallow wells near this dump, risking health problems as in other places (i.e., Adepelumi *et al*. 2005, Samsudin *et al*. 2006). The possibilities of contamination of the aquifer in the landfill area of Oaxaca city are high, since according to studies conducted to evaluate vulnerability to groundwater contamination (Aragón *et al*. 2006), the transit factor of the landfill infiltration ranges from 0.172×10^{-6} to 34.546×10^{-6}/s i.e., over the maximum value, 3×10^{10}/s, established by the Mexican Official Standard (NOM-083-SEMARNAT-2003 in SEMARNAT 2013). This large transit ensures that leachates infiltrate the aquifer with a significant contaminant charge.

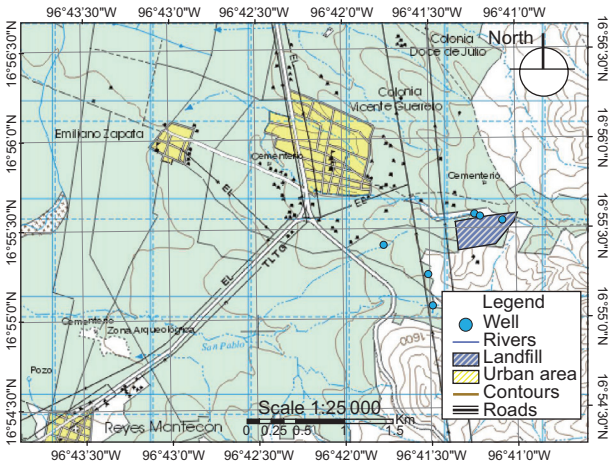

Fig. 1. Location map of the landfill of the Oaxaca city

In this situation, any action taken to diminish the pollution caused by leachates will likely support the economic development of the region. Fortunately, geophysics plays an important role by helping to determine the geometry, spatial extent, and depth of a contamination plume (i.e., Soupios *et al.* 2007). Geophysics has been used to explore the underground and determine if the leachates originated in landfills reached the depth level where the aquifer is found (i.e., Busquets and Casas 1995, Mondelli *et al*. 2007). Among others advantages, geophysical methods are fast and are non-destructive, less expensive than direct methods and provide an overview of the study area. Some authors like Cossu *et al.* (1991) and Soupios *et al*. (2007) report that geophysical methods are favorable for investigation of dumps because they usually contain materials characterized by a high electrical conductivity that can be detected by geoelectrical methods. Karlik (2001) recommended direct current (DC) methods and VLF as tools for mapping groundwater contamination and to determine the extension of the contamination plume.

In this paper we report on the use of two electromagnetic methods, specifically, VLF and EM-LIN (working at low induction numbers similar to EM-34, EM-31 and EM-38 equipments), to evaluate their response in a fractured zone affected by leachates. In the EM-LIN case, measurements were taken in both horizontal and vertical loops modalities for the three separations between the coils allowed by the EM-34. This is equivalent to six measurements for every site, increasing the information obtained from the ground. VLF measurements were taken at three different frequencies in order to select the

ground station with the best coupling with the underground structure.

Hydrogeology of the studied area

The garbage landfill is located in the Atoyac River basin. The runoffs coefficients range between 10 to 20 % and they are favored by the regional topographical slope. The drainage network consists of a basin system through which the superficial runoffs flow intermittently. In this system the landfill plays an important role, since the leachates move permanently to the surface drainage. The number of wells in the area is low and the main groundwater flow direction is toward the southwest (Belmonte *et al.* 2005). The aquifer is free, with the water table located at depths between 6 to 10 m in consolidated and strongly fractured rocks, since due their origin to the tectonic activity of the Oaxaca Fault that controls the regional groundwater flow. There is secondary permeability in some areas.

Electromagnetic prospection at low induction numbers

The EM-LIN method uses two loops, one as source and the other as receiver. The source circulates a current along the coiled wire at a frequency depending on the distance between source and receiver (**Table I**). The source induces a magnetic field with the same frequency into the ground. If both loops are over a whole space, the measurement is predictable and is named primary field (*Hp*). When a half space is present, a secondary field will appear (*Hs*). For a homogeneous half space, *Hs* is known and the rate between both fields is (McNeill 1980):

$$\frac{H_S}{H_P} = \frac{iw\mu_0 \sigma s^2}{4} \qquad (1)$$

Where:

H_S = Secondary magnetic field on the receiver.
H_P = Primary magnetic field on the receiver.

TABLE I. ESTIMATED EXPLORATION DEPTH ACCORDING THE COIL SEPARATIONS AND FREQUENCY USED

Coil separation (m)	Used frequencies (Hz)	Estimated exploration depth (m)	
		Horizontal dipole	Vertical dipole
10	6400	7.5	15
20	2600	15	30
40	600	30	60

$w = 2\pi f$.
f = Frequency in Hz.
μ_0 = Free-space permeability.
σ = Ground conductivity of the homogeneous half space (mS/m).
s = Distance between coils in m.
$i = (-1)^{1/2}$

When the Earth is an inhomogeneous half-space, the conductivity in (1) becomes an apparent one. Using this equipment (EM-34, EM-31, and EM-38 from Geonics and GEM-5 from Geoplex), we can obtain the ground apparent conductivity from the following equation:

$$\sigma_a = 4\frac{\frac{H_S}{H_P}}{\mu_0 w s^2} \qquad (2)$$

Using vertical or horizontal coplanar loops, we can get profiles of apparent conductivity at different separations (corresponding to several penetration depths). Such profiles give us a very broad idea of the conductivity distribution in the ground.

In order to obtain the depth, geometry and true conductivity of the buried body, it is necessary to invert the apparent conductivities. In a two-dimensional Earth (2D), this problem can be posed in terms of the integral equation as the scattering equations. However, we use another integral equation that relates the magnetic fields measured by the receptor and the ground conductivity (Gómez-Treviño 1987). Applying the approximation for low conductivity contrasts, the equation becomes (Pérez-Flores 1995, Pérez-Flores *et al.* 2001):

$$\sigma_a(x_1, x_2) = \frac{|x_1 - x_2|}{\pi} \int_0^{z_f} \int_{x_i}^{x_f} F(x, z, x_1, x_2)\, \sigma(x, z)\, dx dz \qquad (3)$$

Where σ_a is the apparent conductivity obtained from (2) that depends on the source (x_1) and receiver (x_2) positions. If we assume a half-space discretized by a grid of rectangular prisms with center coordinates (x, z), and every prism having a constant conductivity (s), then F constitutes a weighting function. This means that every measurement is a kind of a volumetric average of the product of s's by the corresponding value of F. This function depends on the source and receiver positions, the characteristics of the grid (dimensions) as well as on the magnetic fields induced by the loops. When the loops are horizontally coplanar, this function is:

$$F(x,z,x_1,x_2)= \int_{-\infty}^{\infty} \frac{y^2 + (x-x_1)(x-x_2)}{\sqrt{\left[(x-x_1)^2+y^2+z^2\right]^3\left[(x-x_2)^2+y^2+z^2\right]^3}}\,dy \quad (4)$$

The prisms have infinite extension in the *y* direction. This integral has an analytic solution (Pérez-Flores 1995, Pérez-Flores *et al.* 2001).

For vertical coplanar loops, equation (4) is more complex:

$$F(x,z,x_1,x_2)= \int_{-\infty}^{\infty} \left[E_x(x,y,z,x_1)E_x(x,y,z,x_2) + E_y(x,y,z,x_1)E_y(x,y,z,x_2)\right] dy \quad (5)$$

Where E_x and E_y are the electric fields in the *x* and *y* directions for both, source (x_1) and receiver (x_2). The expressions are developed and explained in Pérez-Flores (1995) and Pérez-Flores *et al.* (2001).

Equation (3) can be expressed as a linear equation system:

$$\overline{\sigma_a} = \mathbf{F}\ \overline{\sigma} \quad (6)$$

Where $\overline{\sigma_a}$ is a vector with the apparent conductivities, **F** is the weighting matrix and σ_a is the vector with the true conductivities of the ground (unknown). This linear system can be solved in many ways. In this work we used quadratic programming (Gill *et al.* 1986) and smoothing factors for the numerical stabilization.

VLF prospecting

VLF instruments are lightweight and portable, and they can be used to study large areas quite quickly (Liu *et al*. 2006). The VLF method is based on the use of very low frequency radio waves (in the range of 15 to 30 kHz) for exploration of fractured zones, groundwater contamination and minerals (Jeng *et al.* 2004, Drahor 2006, Dutta *et al*. 2006, Ganerod *et al*. 2006, Zlotnicki *et al.* 2006, Kaya *et al*. 2007). It helps to determine the electrical characteristics of the underground and shallow rocks (Hutchinson and Barta 2002). There are VLF stations transmitting, for marine communication primary purposes, electromagnetic signals traveling between the ionosphere and the Earth's surface.

The signal emitted by the antennas around the world can be captured in the field by means of VLF instruments, and according to the basic electromagnetic theory, at long distances from the source, the waveform approaches a plane wave (Zlotnicki *et al*. 2006). There is a relation of primary magnetic field (*Hp*) and magnetic secondary field (*Hs*) created by a conductive body that acts as a second source (Kaya *et al*. 2007). This means that electric currents in the conducting body (e.g., a fracture) are generated when radio waves (EM field) pass through it, creating another magnetic field (*Hs*).

The presence of faults and fractures in a hydrogeological system contributes to increase the hydraulic conductivity and porosity acting, in turn, as structures controlling groundwater flow (Sharma and Baranwal 2005, Adepelumi *et al*. 2006). Thus, fractures may also become preferential pathways for the flow of leachate, significantly increasing the electrical conductivity of the subsurface (Mondelli *et al*. 2007, Soupios *et al*. 2007). Depth of penetration depends largely on ground conductivity, but according to Oskooit and Pedersen (2005) this is less than 100 m.

The resulting vector from the sum of *Hp* and *Hs* produces a time-varying elliptically polarized field. This elliptical shape has two components with the same frequency, but different amplitude and phase. The in-phase amplitude *Hp* is the real component, while the out of phase *Hp* is the imaginary component or quadrature component (Eze *et al*. 2004).

The electromagnetic field equation for a conductive medium can be represented by the Helmholtz equation derived from the Maxwell equations:

$$\nabla^2 \begin{Bmatrix} E \\ H \end{Bmatrix} = i\sigma\mu w \begin{Bmatrix} E \\ H \end{Bmatrix} \quad (7)$$

Where *E* and *H* are respectively the electric and magnetic fields, σ (mS/m) the conductivity, μ permeability (Henry / m) and ω the angular frequency.

In contrast, both the tilt angle (θ) and ellipticity (e) are calculated using the formula proposed by Smith and Ward (1974, see also Sharma and Baranwal 2005, and Dutta *et al.* 2006). Once simplified, they are expressed as:

$$\theta = \tan^{-1}\left(\frac{H_s}{H_p} sen\alpha \cos\phi\right) \quad (8)$$

Where *Hp* is the primary field, *Hs* is the secondary field, ϕ is the change of phase between *Hp* and *Hs*.

Hs is tilting, and α represents the angle above *Hp* due to the coupling between the transmitter and the underground structure. Then, it is defined *Hs* sen α = ΔHy, thus equation (8) becomes.

$$\theta = \tan^{-1}\left(\frac{\Delta H_y}{H_p}\cos\phi\right) \quad (9)$$

Where $\Delta H_y \cos\phi$ = real component or in-phase of the *Hs* field.

The tangent of the tilt angle is proportional to the *Hs* real component, which is measured in the vertical direction. Therefore, the measurement of the tilt angle is very similar to measuring the real component (in-phase) of *Hs* in the vertical direction.

VLF data can be enhanced by applying filtering procedures. The filter application is essential to obtain a reasonable correlation between the anomaly and the structure. The filters are designed to decrease noise from the EM signal. Fraser, as well as Karous and Hjelt filters, are two methods widely used in VLF data processing.

Fraser filter is a low-pass function for estimating the average of tilt angle measurements produced by a subsurface conductor. In a linear sequence of tilt angle measurements M_1, M_2, M_3, ..., M_n, the Fraser filter F_1 is expressed as:

$$F_1 = (M_3 + M_4) - (M_1 + M_2) \quad (10)$$

The first value F_1 is located between M_2 and M_3 positions, the second value between M_3 and M_4, and so on. There are several studies using Fraser filter (Adepelumi *et al*. 2005, Cossu *et al*. 1991, Liu *et al*. 2006, Monteiro-Santos *et al.* 2006, Zlotnicki *et al.* 2006).

Karous and Hjelt (1983) developed a statistical linear filter, based on Fraser´s one, which provides a profile of current density vs. depth (H_0) and is derived from the magnitude of the vertical component of the magnetic field (*Hz*) in a specific position. These authors used linear filtering for the analysis of VLF dip-angle data in an extension of the Fraser filter.

They describe the magnetic field, arising from a subsurface 2D current distribution, assumed in a thin horizontal sheet of varying current density situated everywhere at a depth equal to the distance between the measurement stations. Their technique involves filtering the same data set for various depths and gives an idea about the conductivity with depth, since high current density corresponds to good conductors. This technique has found wide popularity as it provides a simple, readily implemented scheme for semi-quantitative analysis and target visualization. The apparent current density pseudo section should provide a pictorial indication of the depths of various current concentrations and hence the spatial distribution of subsurface geologic features (Ogilvy and Lee 1991).

When we measure over conductors, the in-phase part of the equivalent current distribution has only positive values. Negative parts on both sides of the conductor can be caused either by the length of the filter or by a decrease of current density due to current gathering which is not present in 2D structures (Nabighian 1982). In the simplest form, the Fraser filter is:

$$\frac{\Delta z}{2\pi} I_a(\Delta x/2) = -0.205H_{-2} + 0.323H_{-1} - 1.446H_0 + 1.446H_1 - 0.323H_2 + 0.205H_3 I_a(\Delta x/2) \quad (11)$$

Where Δz is the assumed thickness of the current sheet, I_a, is the current density, x the distance between data points and also the depth to the current sheet. The H_2 through H_3 values are the normalized vertical magnetic field anomalies at each set of six points. The location of the calculated current density is assumed at the geometrical center of the six data points (Sundararajan *et al.* 2007).

METHODOLOGY

Measurements were conducted along six profiles with the EM-LIN and VLF methods; four profiles are common for both methods, respective lengths of 325, 320, 300 and 645 m (**Fig. 2**). Three profiles were made in the southern side, one on the northern side of the landfill with E-W direction. Two additional

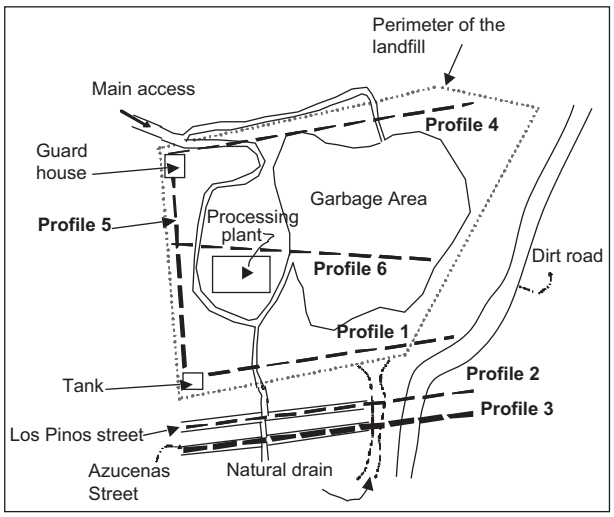

Fig. 2. Location of the studied profiles. Profiles 1 to 4 were measured with EM-LIN, 5 and 6 profiles only with VLF

VLF profiles were made: one in the middle part of the landfill with E-W direction. The other one on the western side, with a N-S direction: lengths respectively of 415 and 275 m. In all cases the measurements were made every 5 m.

Structural features from rock outcrops, fracture degree and its preferred direction were also measured. For the topographic survey, an Ashtech Promark GPS post processing equipment was used.

The VLF survey was done with a Scintrex equipment with transmitting signals from three stations: NAU located in Aguada, Puerto Rico, with a frequency of 28.5 kHz; NPM located in Lualualei, Hawaii, with a frequency of 23.4 kHz and NSS located in Annapolis, Maryland, USA, with a frequency of 21.4 kHz. For the respective data processing, the software KHFFILT-2006 was used (prepared by Pirttijärvi 2004), to apply the Karous and Hjelt (1983) and Fraser (1969) filtering to VLF data.

The control source electromagnetic data were measured with an EM-LIN equipment (Geonics), consisting of transmitter and receiver coils; performing measurements with three different intercoil spacing (10, 20 and 40 m) at different frequencies (6400, 2600, and 600 Hz) respectively, and in two forms: horizontal coplanar coils (vertical magnetic dipole) and vertical coplanar coils (horizontal magnetic dipole). Data processing for the electromagnetic coils method were performed using the software CICEM35-2006. This program applies the theory developed by Pérez-Flores (1995) and Pérez-Flores *et al.* (2001) for the EM data inversion, which considers the measurements obtained with EM-34 equipment as a weighted average of the earth conductivity distribution.

ANALYSIS AND DISCUSSION OF THE RESULTS

The electromagnetic LIN array comprised several source-receiver separations. For horizontal and vertical coplanar loops, we obtained four pseudo-sections (images) of the apparent conductivity (mS/m) along the profiles comprising several studied depths. **Figure 3** shows, as an example, for profile 1, for a vertical dipole (**Fig. 3a**) as well as for a horizontal dipole (**Fig. 3b**), the behavior of electrical conductivity along the profile, for different depths.

The six data sets for profile 1 are different because every array looks at the ground in a different way (**Fig. 3**). However, they show a general behavior that can give us a very broad idea of the conductivity

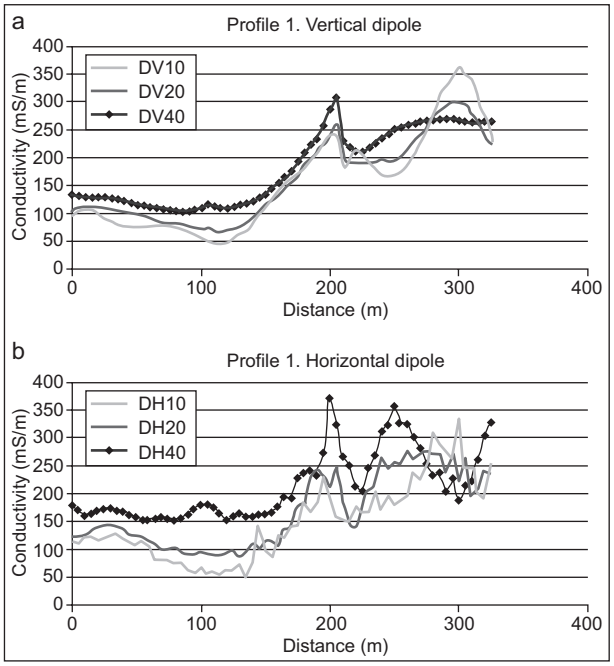

Fig. 3. Behavior of electrical conductivity along profile 1. a) vertical dipole, and b) horizontal dipole

variation with depth and horizontally. The observed conductors are assumed to be related with conductive materials like contaminant fluids contained in the porous media. In order to merge those six data sets to get one conductivity model or image of the ground conductivity, we joint inverted them into a model whose response fits the six data sets very well (Pérez-Flores *et al.* 2001). In **figure 4** are shown the conductivity images or models for the four EM-LIN profiles located in **figure 2**.

Regarding the VLF data, only the in-phase component was processed. **Figure 5** shows the behavior of the in-phase and quadrature curves for profile 1 in order to illustrate the data collected in field.

The interpretation of VLF data was based on filtering procedures following Fraser (1969) and Karous and Hjelt (1983) methods widely used by other authors (i.e., Benson *et al*. 1997, Sundararajan *et al*. 2007). Fraser filter turns the crossing points into peak signals that enhance the conductive structures. In **figure 6** for profile 1, we can appreciate the results of Fraser filter, showing the percentage (%) in the y-axis. In particular a significant negative value can be observed at position 125 m due to changes in the underground conductivity. Karous and Hjelt (1983) filtering was used to obtain current density pseudo-sections (mA/cm^2) for the six VLF profiles (**Fig. 7**). Processed data are presented with iso-contour lines of current density. Low current density values correspond to high resistivity values.

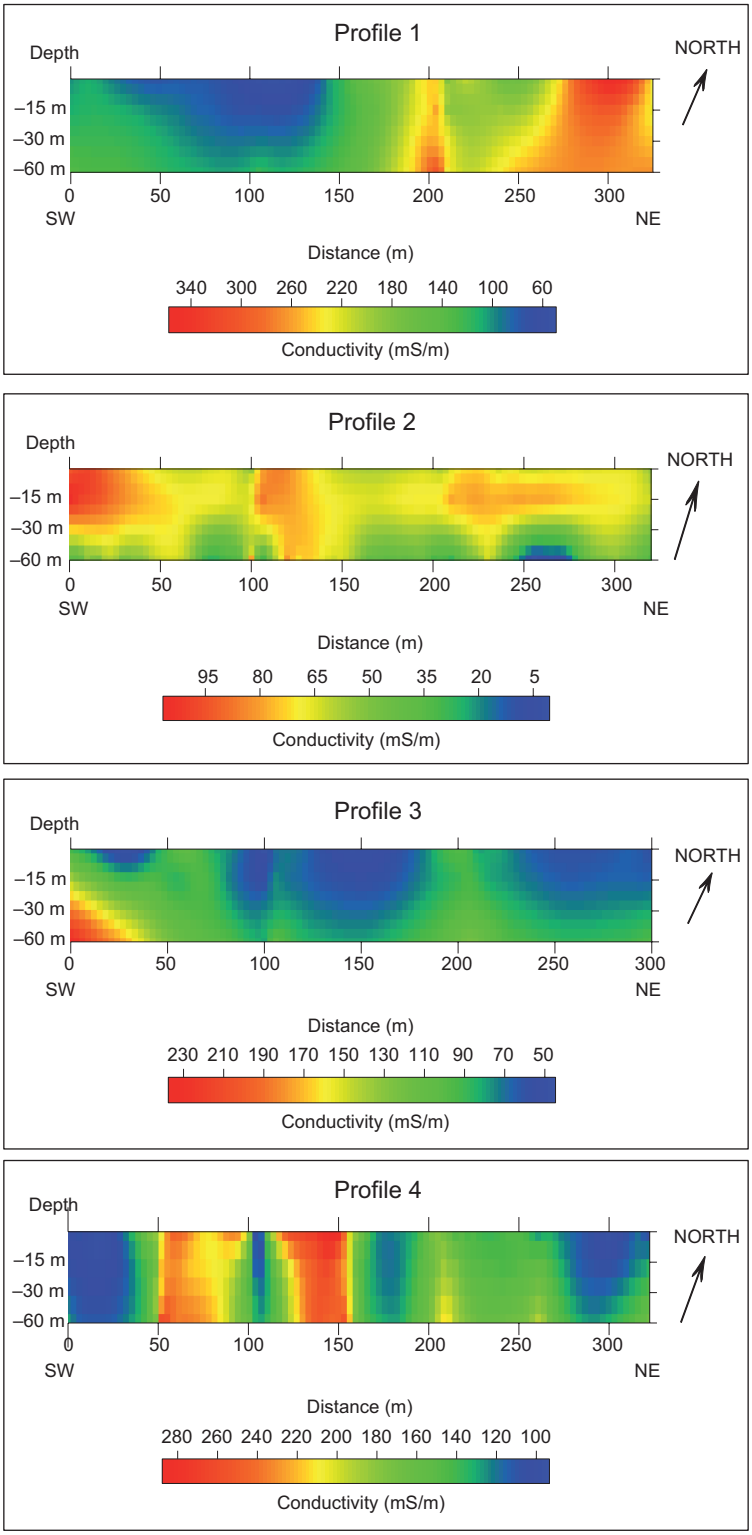

Fig. 4. 2D sections obtained by data inversion. See **Fig. 2** for location of profiles

By correlating the EM-LIN conductivity image with the corresponding VLF current density pseudo-section, it is possible to construct a geological-geophysical model for every profile. In the following interpretation, only anomalies well defined by several neighboring assignment points were taken into

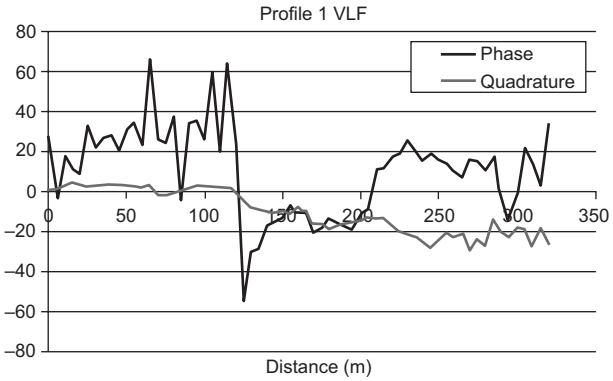

Fig. 5. Behavior of the in-phase and quadrature of profile 1

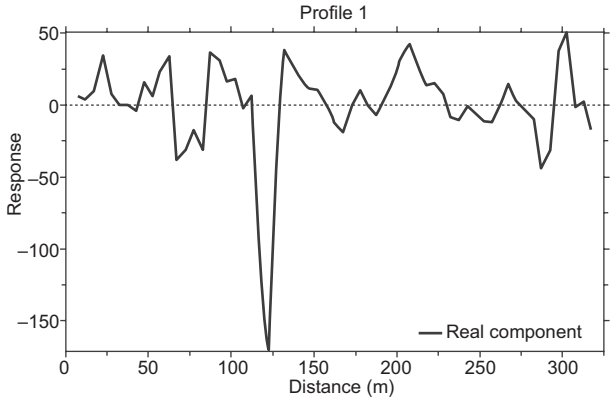

Fig. 6. Profile 1 where the real component or phase is processed by the Fraser Filter

account (i.e., anomalies defined by several contiguous points along the horizontal and along the vertical). Also anomalies located at the upper end points were not considered (i.e., only the middle portion). In general there is a fair-to-good agreement between conductivity zones imaged by the EM-LIN inversion, and the areas of high current density obtained from the VLF data. Each of the high conductivity zones interpreted and reported below is supported by both data sets types, as well as by the presence at surface of leachates.

Along profile 1 (**Fig. 8**), located near the southern perimeter of the landfill, two conductive zones are observed at the central part (at 200 m, and around 300 m), which are the most important in terms of spatial distribution (see **Fig. 4a**). The anomaly at 200 m is also represented as current density anomalies (**Fig. 7c**), thereby it is interpreted as a fracture zone. In the VLF section a narrow anomaly is observed around 150 m, which is also assumed a fracture zone. Both zones lie below a local topographic depression (see profiles 2 and 3), and below the surficial leachate flow. The

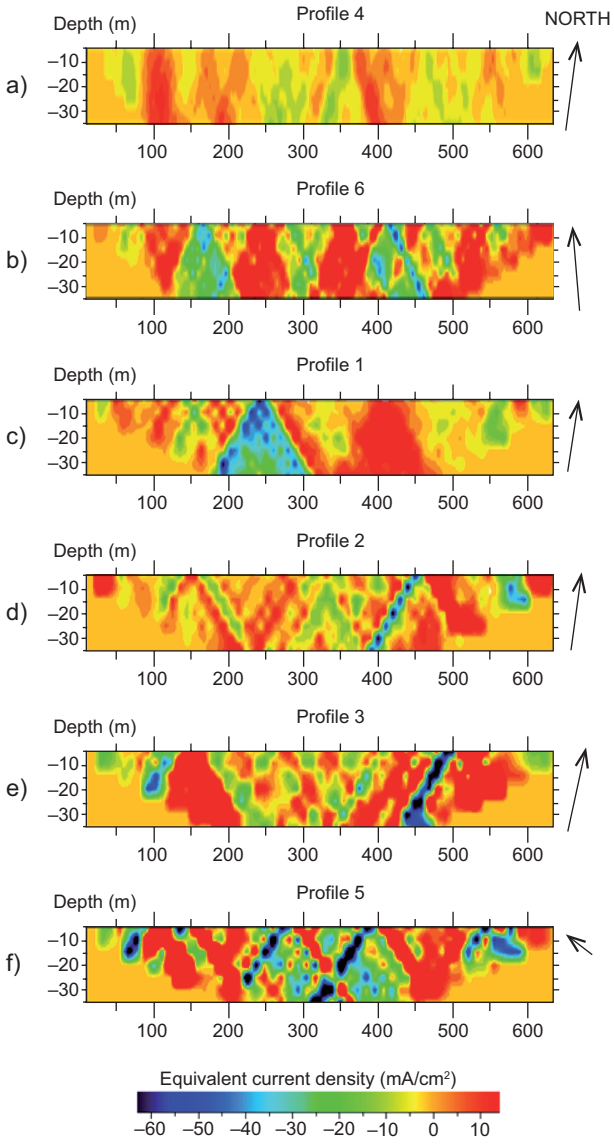

Fig. 7. a, b, c, d, e and f. VLF profiles processed with Karous-Hjelt filter. The scale of values represents the current density (mA/cm^2), associating positive values to conductive areas because of the content of leachate seeping into the fractured medium

topography is irregular, the geology is represented by alternations of sandstone-fractured shale.

The geological-geophysical model associated with profile 2 (**Fig. 9**), which is located outside the landfill, to the south of profile 1, shows three major conductive zones (between 0 and 50 m, between 100 and 150 m, and between 200 and 300 m) (**Fig. 4b**). According to VLF, there is a fracture zone between 225 and 275 m (i.e., correlating with the third conductive zone) (**Fig. 7d**). Another fracture zone might be located around 175 m. The third conductive anomaly is associated with the presence of fractures with N-S

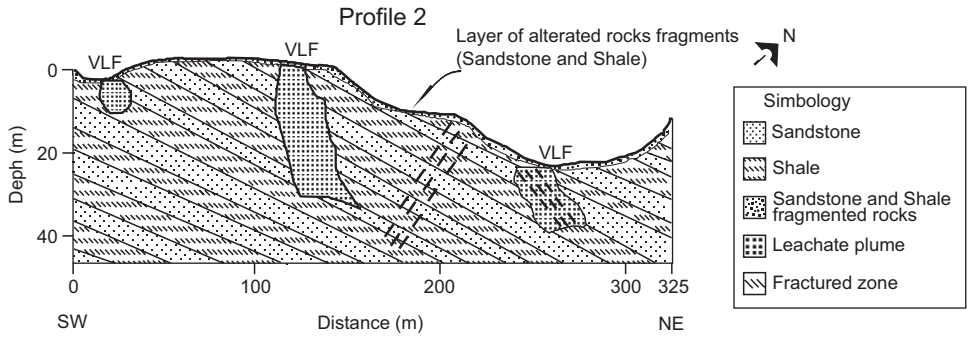

Fig. 8. Geological model along profile 1, with superposed leachate presence inferred by LIN and fractures by VLF EM methods.

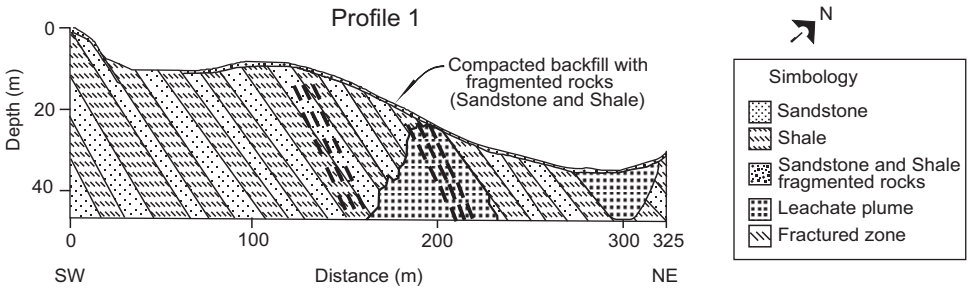

Fig. 9. Geological model along profile 2, with superposed leachate presence inferred by LIN and fractures by VLF EM methods.

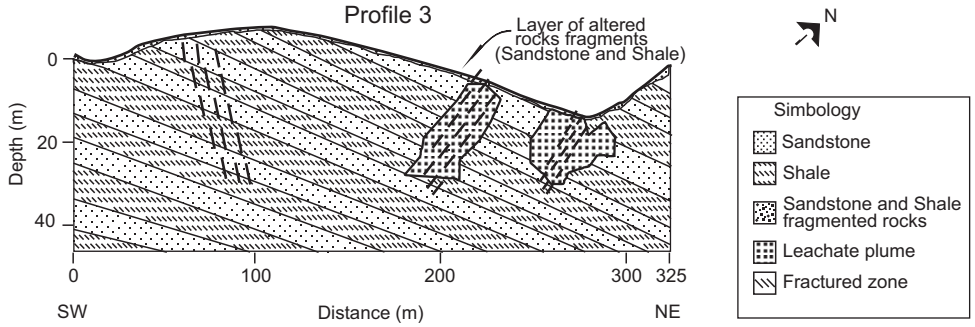

Fig. 10. Geological model along profile 3, with superposed leachate presence inferred by LIN and fractures by VLF EM methods

direction (and in a lesser proportion with an E-W orientation), through which leachates are infiltrating. The anomalies have a lesser vertical extension.

The topography is not flat. There is a topographic local depression at the eastern half, and the ground comprises an alternation of shale and sandstone with a surface layer of the same materials but altered and weathered.

Profile 3 (**Fig. 10**), located outside the landfill, to the south of profile 2, presents only a minor feature that can be associated with the presence of leachates at the subsurface (**Fig. 4c**; around 200 m). This indicates that the contaminant plume does not continue southwards, or it has deepened and it can not be sensed due to the limited penetrating power of the two used methods. VLF indicates the possible existence of three fractures zones (between 50 and 100 m, around 200 m, and another centered in 250 m; **Fig. 7e**). The last fracture would be located below the surficial leachates flow, and would point to the infiltration of leachate into the ground through it, and can be interpreted as a leachate plume. Geologically, this profile consists of a thin layer of sand-shale rock fragments and then alternation of shale and sandstones.

Figure 11 shows the geological-geophysical model for profile 4, which is the longest and located in the northern portion of the landfill in an area where

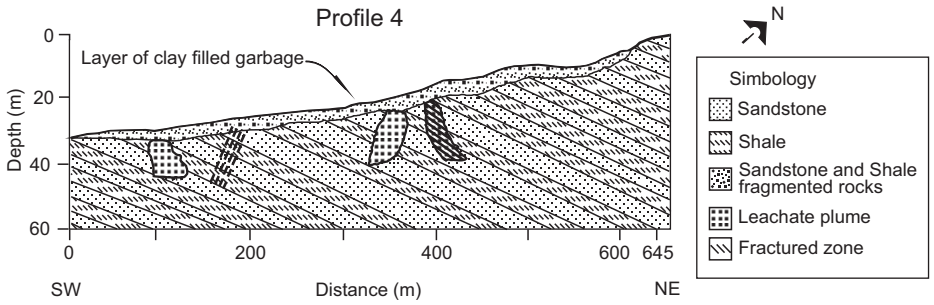

Fig. 11. Geological model along profile 4, with superposed leachate presence inferred by LIN and fractures by VLF EM methods

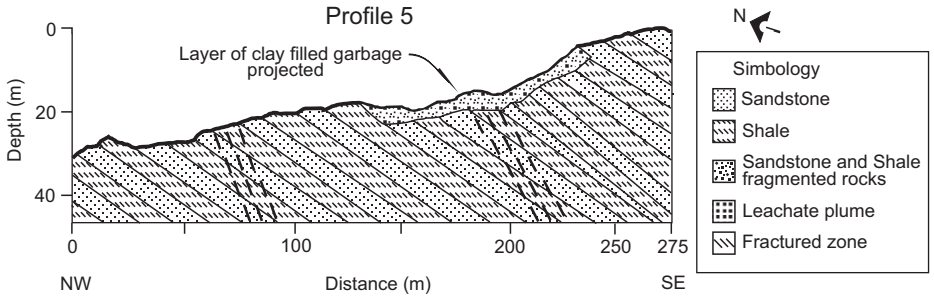

Fig. 12. Geological model along profile 5, with superposed leachate presence inferred by LIN and fractures by VLF EM methods

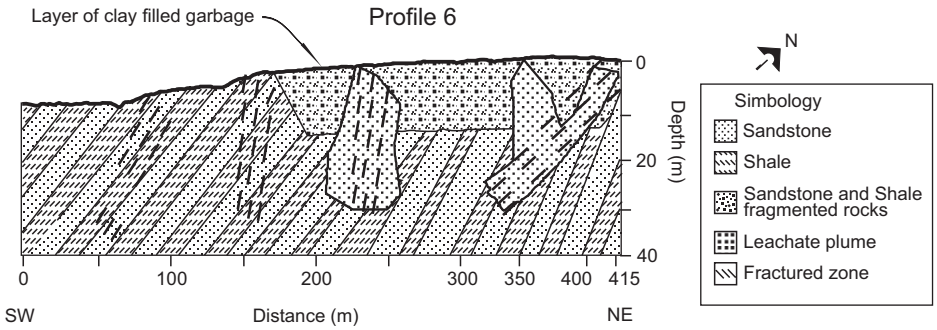

Fig. 13. Geological model along profile 6, with superposed leachate presence inferred by LIN and fractures by VLF EM methods

in the past waste was deposited but not anymore. Two anomalies are mapped at 100, extending from 250 and towards 300 m (**Fig. 4d**). Two relative anomalies are observed between 375 and 425 m. VLF indicates fractures centered at 200 and at 400 m (**Fig. 4a**), correlating with the second conductive zone. At field, leachates were observed percolating through these fractures.

The geological-geophysical model of the profile 5 is presented in **figure 12**, where two zones with high current density are interpreted as fractures (at 85 m, and one centered at 200 m; **Fig. 7f**). Onto this profile is projected the location of the main body of garbage with a clay filling in the middle of it, and with leachates observed at its surface and whose spatial distribution was obtained from VLF and EM-LIN measurements along profiles 1, 2, 3, 4, and 6. The geology corresponds to an alternation of shale-sandstone. This profile is located in the western part of the landfill.

Figure 13 corresponds to the geological-geophysical model of the profile 6. This profile was conducted at the center of the landfill, so almost half of it is over a layer of garbage with a thickness from 10 to 15 m of depth. VLF indicates the presence of four possible fracture zones (at 65 m, at 150 m, at 225 m, and between 300 and 400 m) (**Fig. 7b**). It sounds logic to suppose that through the two easternmost fractures leachates percolates, since they are located below the local topographic depression where the

maximum thickness of wastes is located. The geology is represented by an alternation of fractured shale and sandstone.

The analysis of all the models shows that the conductive areas are related to the presence of leachates and may suggest a continuous flow of them through the landfill of Oaxaca city, and also that the subsurface layers are being impregnated with this contaminant flow through the fractures up to depths of more than 30 m.

Figure 14 shows interpolated images of apparent conductivity measured with the EM-LIN considering the respective four profiles, in the configuration-modality of horizontal coplanar coils (vertical dipole). It can be observed that at different depths, the contaminant plume is larger in the N-S preferential direction of the leachate flow. We can observe that the high conductivity anomaly correlates with the landfill limits. Fractures inferred from VLF data are superposed. Two fracture systems can be observed to run with a NW-SE direction.

CONCLUSIONS

The Oaxaca city garbage landfill is located in a fractured zone where the VLF and EM-LIN electromagnetic geophysical methods were applied to study the presence of leachates in the subsoil. Accordingly, the preferential flow of leachates is through the set of NW-SE fractures. We defined their spatial distribution. The data obtained from EM-LIN coils show high conductivity zones, interpreted to be due to the presence of leachates. From the information

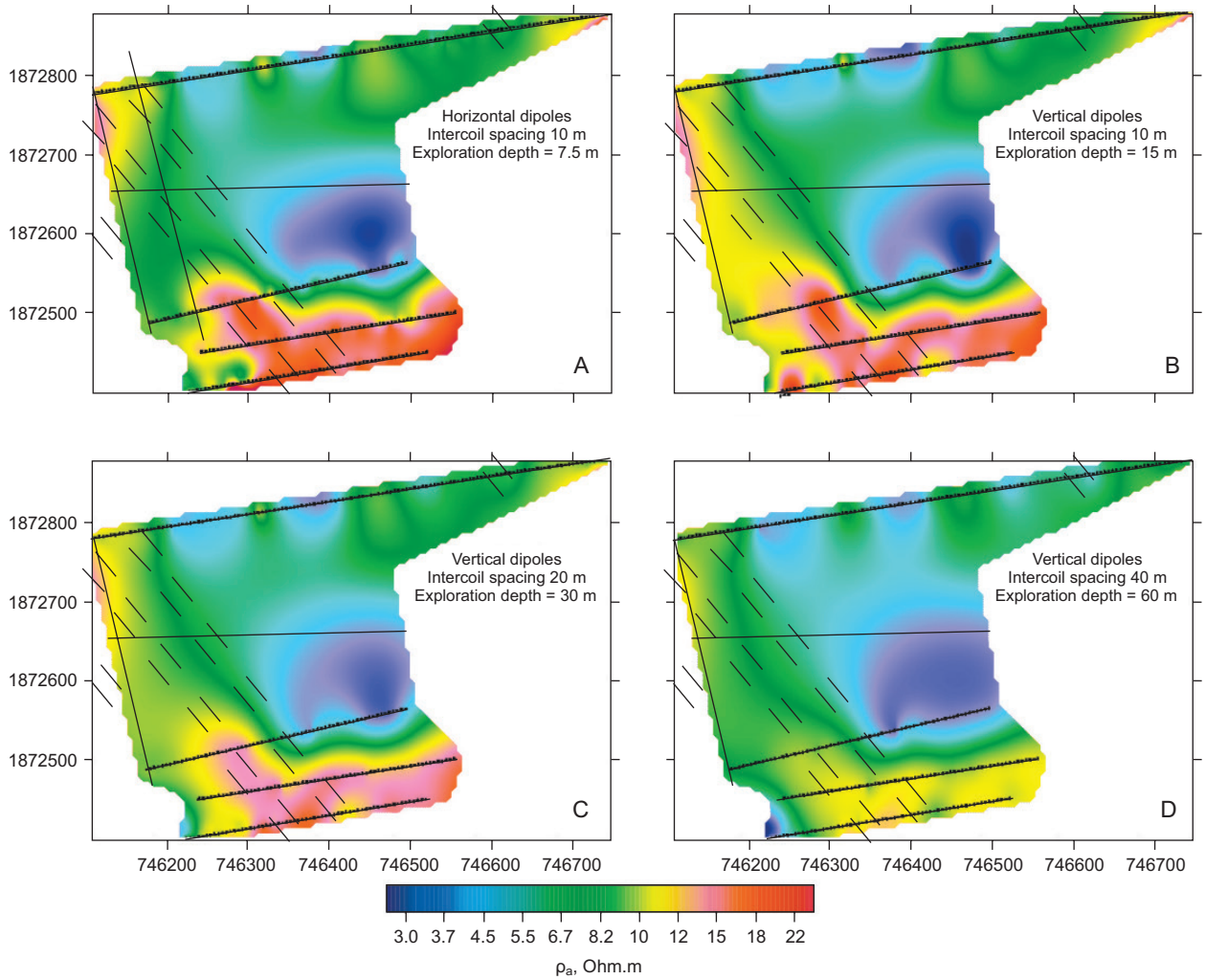

Fig. 14. Perspective at different depths for the EM coils processed data, corresponding to the horizontal (A) and vertical (B, C, and D) dipole mode

obtained from the VLF method (in-phase component) about 13 fractured zones were identified along the studied profiles, favoring the leachate percolation through the fractured zone. In general, there is a good correlation between high conductivity areas obtained with EM-LIN and those high current densities obtained with VLF.

Considering that the water table of the surrounding areas is located at a depth less than 15 m, there are high possibilities that the aquifer could be contaminated. In the outskirts of the landfill there is a semi-confined aquifer, however, the fractures favor leachates flowing inside the area, allowing the leachate to infiltrate to greater depths. There are anomalous conductive areas with depths varying from 60 to 35 m in the case of EM-LIN and VLF method of coils respectively.

Finally, it is considered that the use of these two methods (VLF and EM-LIN) for the detection of leachates in the subsoil is suitable as a technique for assessment of contaminated areas. It is faster than other geophysical methods and not invasive.

REFERENCES

Adepelumi A.A., Ako B.D., Afolabi O. y Arubayi J.B. (2005). Delineation of contamination plume around oxidation sewage-ponds in Southwestern Nigeria. Environ. Geol. 48, 1137-1146.

Adepelumi A.A., Yi M. J., Kim J.H., Ako B.D. y Son J.S. (2006). Integration of surface geophysical methods for fracture detection in crystalline bedrocks of southwestern Nigeria. Hydrogeol. J. 14, 1284-1306.

Aragón S. M., Belmonte J. S. I. y Navarro M. S (2006). Vulnerabilidad del acuífero del tiradero municipal de la ciudad de Oaxaca a la contaminación subterránea. Memorias. XV Congreso Nacional de Ingeniería Sanitaria y Ciencias Ambientales. Guadalajara, Jal. 24 al 26 de mayo, 2006. CD-ROM.

Belmonte-Jiménez S.I., Campos-Enríquez J.O. y Alatorre-Zamora M.A. (2005). Vulnerability to contamination of the Zaachila aquifer, Oaxaca, Mexico. Geofís. Int. 44, 283-300.

Benson A.K., Payne K.L. y Stubben M. A. (1997). Mapping groundwater contamination using dc resistivity and VLF geophysical methods - A case study. Geophysics 62, 80-86.

Busquets E. y Casas, A. (1995). Caracterización de vertederos y detección de penachos contaminantes mediante la utilización de métodos geofísicos. Física de la Tierra (Servicio de Publicaciones de la Universidad de Complutense) 7, 207-226.

Cossu R., Ranieri G., Marchisio M., Sambuelli L., Godio A. y Motzo G.M. (1991). Geophysical methods in surveying old landfills. Proceedings of the Contaminated soil '90 Third International KfK/TNO Conference. Karlsruhe, Federal Republic of Germany. December 10-14. I, 575-582.

Drahor M.G. (2006). Integrated geophysical studies in the upper part of Sardis archaeological site, Turkey. J. Appl. Geophys. 59, 205-223.

Dutta S., Krishnamurthy N.S., Arora T., Rao V.A., Ahmed S., y Baltassat J.M. (2006). Localization of water bearing fractured zones in a hard rock area using integrated geophysical techniques in Andhra Pradesh, India. Hydrogeol. J. 14, 760-766.

Eze C.L., Mamah L.I., y Israel-Cookey C. (2004). Very low frequency electromagnetic (VLF-EM) response from a lead sulphide lode in the Abakaliki lead/zinc field, Nigeria. Int. J. Appl. Earth Obs. Geoinformation 5, 159-163.

Fraser D.C. (1969). Contouring of VLF-EM data. Geophysics 34, 958-967.

Ganerød G. V., Rønning J.S., Dalsegg E., Elvebakk H., Holmøy K., Nilsen B. y Braathen A. (2006). Comparison of geophysical methods for sub-surface mapping of faults and fracture zones in a section of the Viggja road tunnel, Norway. Bull. Eng. Geol. Environ. 65, 231-243.

Gill P.H.S., Murray W., Saunders M. y Wright M. (1986). User's guide for LSSOL: A package for constrained linear least-square and quadratic programming. Stanford University. Technical Report SOL-886-1. EUA.

Gomez-Trevino E. (1987). Nonlinear integral equations for electromagnetic inverse problems. Geophysics 52, 1297-1302.

Hutchinson P.J. y Barta L.S. (2002). VLF surveying to delineate longwall mine-induced fractures. Leading Edge 21, 491-493.

Jeng Y., Lin M.J. y Chen C.S. (2004). A very low frequency-electromagnetic study of the geo-environmental hazardous areas in Taiwan. Environ. Geol. 46, 784-795.

Karlik G. y Kaya M. A. (2001). Investigation of groundwater contamination using electric and electromagnetic methods at an open waste-disposal site: A case study from Isparta, Turkey. Environ. Geol. 40, 725-731.

Karous M. y Hjelt S.E. (1983). Linear filtering of VLF dip-angle measurements. Geophys. Prospect. 31, 782-794.

Kaya M.A., Özürlan G. y Şengül E. (2007). Delineation of soil and groundwater contamination using geophysical methods at a waste disposal site in Çanakkale, Turkey. Environ. Monit. Assess. 135, 441-446.

Liu H., Liu J., Yu C., Ye J. y Zeng Q. (2006). Integrated geological and geophysical exploration for concealed ores beneath cover in the Chaihulanzi goldfield, northern China. Geophys. Prospect. 54, 605-621.

McNeill J.D. (1980). Electromagnetic terrain conductivity measurements at low induction numbers. Technical Note TN-6, Geonics Ltd. Mississauga, Canada.

Mondelli G., Giacheti H., Boscov M., Elis V. y Hamada J. (2007). Geoenvironmental site investigation using different techniques in a municipal solid waste disposal site in Brazil. Environ. Geol. 52, 871-887.

Monteiro-Santos F.A., Mateus A., Figueiras J. y Gonçalves M.A. (2006). Mapping groundwater contamination around a landfill facility using the VLF-EM method - A case study. J. Appl. Geophys. 60, 115-125.

Nabighian M.N. (1982). A review of time-domain electromagnetic exploration. In: Proceedings of the International Symposium of Applied Geophysics in Tropical Regions (J. Seixas Lourenço, L. Rijo, Eds). Conselho Nacional de Desenvolvimento Científico e Tecnológico. Belem, Brazil, September l-8.

Ogilvy R.D. y Lee A.C. (1991). Interpretation of vlf-em in-phase data using current density pseudosections. Geophys. Prospect. 39, 567-580.

Oskooi B. y Pedersen L.B. (2005). Comparison between VLF and RMT methods. A combined tool for mapping conductivity changes in the sedimentary cover. J. Appl. Geophys. 57, 227-241.

Pérez-Flores M.A. (1995). Inversión rápida en 2-D de datos de resistividad, magnetotelúricos y electromagnéticos de fuente controlada a bajos números de inducción. Ph. D. Thesis. Centro de Investigación Científica y de Educación Superior de Ensenada. Baja California, México. 352 pp.

Pérez-Flores M.A., Méndez-Delgado S. y Gómez-Treviño E. (2001). Imaging low-frequency and dc electromagnetic fields using a simple linear approximation. Geophysics 66, 1067-1081.

Pirttijärvi M. (2004). KHFfilt program. A geophysical software for Karous-Hjelt and Fraser filtering on geophysical VLF (very-low-frequency) data. Geopysics Division, Department of Geosciences, University of Oulu, Finland.

Samsudin A., E. B., Zurairi W., Hamzah U. (2006). Mapping of contamination plumes at municipal solid waste disponsal sites using geoelectric imaging technique: case studies in Malaysia. J. Spat. Hydrol. 6, 13-22.

SEMARNAT (2003). Norma Oficial Mexicana NOM-083-SEMARNAT-2003. Especificaciones de protección ambiental para la selección del sitio, diseño, construcción y operación, monitoreo, clausura y obras complementarias de un sitio de disposición final de residuos sólidos urbanos y de manejo especial. Secretaría de Medio Ambiente, Recursos Naturales y Pesca. Diario Oficial de la Federación. 20 de octubre de 2004.

Sharma S.P. y Baranwal V.C. (2005). Delineation of groundwater-bearing fracture zones in a hard rock area integrating very low frequency electromagnetic and resistivity data. J. Appl. Geophys. 57, 155-166.

Smith B.D. y Ward S.H. (1974). On the computation of polarization ellipse parameters. Geophysics 39, 867-869.

Soupios P., Papadopoulos N., Papadopoulos I., Kouli M., Vallianatos F., Sarris A. y Manios T. (2007). Application of integrated methods in mapping waste disposal areas. Environ. Geol. 53, 661-675.

Sundararajan N., Nandakumar G., Narsimha M., Ramam K. y Srinivas Y. (2007). VES and VLF - An application to groundwater exploration, Khammam, India. Leading Edge 26, 708-716.

Zlotnicki J., Vargemezis G., Mille A., Bruère F. y Hammouya G. (2006). State of the hydrothermal activity of Soufrière of Guadeloupe volcano inferred by VLF surveys. J. Appl. Geophys. 58, 265-279.